Chemicals and reagents

Chemicals such as 3-methoxy-salicylaldehyde (*o*-vanillin), 2-hydroxy-1,3-diaminopropane, $Eu(NO_3)_3$, $La(NO_3)_3$ (Aldrich), $Cu(NO_3)_2$ and triethylamine (TEA) (Merck, India) are of reagent grade and used without further purification. Solvents like methanol, ethanol (Merck, India) were of reagent grade and used as received. The Schiff base ligand (H_3L) was prepared as reported elsewhere.[1]

Synthesis of $[Cu^{II}Eu^{III}(HL)(H_2O)(NO_3)_3]$(1)

A 20 cm^3 methanol solution of $Cu(NO_3)_2{\cdot}6H_2O$ (0.263 g, 1.0 mmol) was added to a solution of H_3L (0.358 g, 1.0 mmol) containing triethylamine (TEA) (0.201 g, 2.0 mmol) in methanol (30 cm^3) at room temperature under constant stirring. The resulting mixture is stirred for 10 min, and then finely powdered europium nitrate $Eu(NO_3)_3$ (0.446 g, 1.0 mmol) was added After being stirred for 1h, the mixture was filtered to remove the precipitate, if any, and the clear green filtrate is then kept for slow evaporation. After a few days, green single crystals, suitable for X-ray diffraction were precipitated out, which were then collected by filtration and washed with cold methanol. Colour: Dark green. Yield: 0.557 g (72%). IR: 1619 vs cm^{-1} for ν(C=N), 3134 cm^{-1} for ν(alcoholic –OH); ν(nitrate) 1449s, 1322s. *Anal. calcd.* (%) for $C_{19}H_{22}CuEuN_5O_{15}$: C 29.40, H 2.86, N 9.03. Found: C 29.68, H 3.68, N 9.17.

Synthesis of $[Cu^{II}La^{III}(HL)(H_2O)(NO_3)_3]$(2)

The complex **2** was synthesized the same procedure as described above for **1**, except using the appropriate metal salt $Ln(NO_3)_3.6H_2O$ for **2**. Colour: Dark green. Yield: 0.494 g (65%). IR: 1656 vs cm^{-1} for ν(C=N), 3025 cm^{-1} for ν(alcoholic –OH); ν(nitrate) 1509s, 1386s. Mr = 762.85. *Anal. calcd.* (%) for $C_{19}H_{22}CuN_5O_{15}La$: C 29.90, H 2.91, N 9.18. Found: C 29.44, H 3.28, N 8.95.

Physical measurements

Elemental analyses were carried out using an automated elemental analyzer (Perkin-Elmer 240). IR spectrum (400 – 4000 cm^{-1}) was recorded in KBr pellets using FTIR spectrometer (Magna IR 750 series-II, Nicolet).

Crystallography

Single crystal X-ray data of complex **1** and **2** were collected on a CCD diffractometer (SMART APEX-II, Bruker) using graphite monochromated Mo-K_α radiation of λ = 0.71073 Å. The Bruker Apex-II suite program was used for the collection of data and subsequent, reduction, structure solution. All available reflections to $2\theta_{max}$ are harvested and corrected for Lorentz and polarization factors with SAINT plus.[2] Reflections were then corrected for absorption, interframe scaling, and other systematic errors with SADABS.[2] The solution of structures were performed adopting the direct methods and then refined by means of full matrix least-square technique based on F^2 with SHELX-97.[3] All the non-hydrogen atoms were refined with anisotropic thermal parameters. All hydrogen atoms on carbons are placed on their geometrically idealized positions, while hydrogen atom on the free –OH group was found on the difference Furrier map, and all of them were constrained to ride on their parent atoms. The crystallographic data for **1** and **2** is given in Table S1.

Magnetometry

Temperature dependence of the DC magnetization was measured with a SQUID magnetometer (MPMS-XL7, Quantum Design) using the RSO mode of detection. For magnetic susceptibility the applied field was B_{DC} = 0.5 T; data were corrected for the underlying diamagnetism and converted to the effective magnetic moment. AC susceptibility measurements were conducted with the amplitude B_{AC} = 0.38 mT and ten scans were averaged.

Table S1 Crystallographic data and details of the structure determination for **1** and **2.**

Molecular formula	$C_{19}H_{20}CuEuN_5O_{15}$ (**1**)	$C_{19}H_{20}Cu\ LaN_5O_{15}$ (**2**)
Formula Weight	773.92 + 2H	760.86 + 2H
Crystal System	Monoclinic	Monoclinic
Space group	$P2_1/c$ (No. 14)	$P2_1/c$ (No. 14)
a /Å	9.0405(6)	9.0598(5)
b /Å	28.426(2)	28.5710(14)
c /Å	10.3509(9)	10.3072(5)
α /deg	90	90
β /deg	105.248(3)	105.404(5)
γ /deg	90	90
V /Å^3	2566.4(3)	2572.2(2)
Z	4	4
D(calc) /g cm^{-3}	2.003	1.965
μ(MoK$_\alpha$) /mm^{-1}	3.335	2.550
F(000)	1524	1500
T /K	273	293
θ min, max /deg	1.4, 27.5	3.0, 29.2
Dataset	-11: 11 ; -36: 36 ; -13: 13	-11: 12 ; -38: 38 ; -13: 12
Tot., Uniq. Data, R(int)	11855, 5906, 0.042	26736, 6246, 0.042
Observed data [$I > 2\sigma(I)$]	4726	5403
N_{ref}, N_{par}	5906, 373	6246, 373
R, wR_2, S	0.0729, 0.1794, 1.05	0.0645, 0.1831, 1.02
CCDC No	**1528225**	**1535826**

Table S2. Hydrogen bonding interactions in **1** (Å, º).

D−H•••A	Distances (Å)			Angles (º)
	D−H	H•••A	D•••A	D−H•••A
O6 -H6 •••O11^{i}	0.82	2.12	2.817(14)	143
C1 –H2B •••O10	0.96	2.37	2.826(16)	109
C1 –H2C •••O6^{ii}	0.96	2.58	3.369(17)	139
C14 -H7 •••O9^{iii}	0.93	2.47	3.367(16)	163
C19 –H11B •••O11	0.96	2.49	3.034(16)	116
C19 -H11C•••O5^{iv}	0.96	2.52	3.405(15)	153
C3 –H20 •••O14^{v}	0.93	2.52	3.321(16)	144

Symmetry code: (i) = x,y,-1+z; (ii) = 1+x,y,1+z; (iii) = -1+x,3/2-y,-1/2+z; (iv) = x,3/2-y,1/2+z; (v) = 1+x,y,z.

Table S3. Hydrogen bonding interactions in **2** (Å, º).

D−H•••A	Distances (Å)			Angles (º)
	D−H	H•••A	D•••A	D−H•••A
O16 –H36 •••O8^{i}	0.82	2.54	2.841(16)	103
C13-H13•••O7 ^{ii}	0.93	2.46	3.351(15)	159
C19-H19•••O12^{iii}	0.93	2.60	3.492(14)	161
C22-H22A•••O16^{iv}	0.96	2.56	3.350(17)	139
C23-H23•••O11^{v}	0.93	2.53	3.319(16)	143
O16 –H36•••O15	0.82	2.37	3.111(16)	151

Symmetry code: (i) = x,y,-1+z; (ii) = -1+x,1/2-y,-1/2+z; (iii) = 1-x,-y,-z; (iv) = 1+x,y,1+z; (v) = 1+x,y,z.

Table S4. Selected bond lengths (Å) and bond angles (°) in **1** and **2**

1				**2**			
Eu1–O1	2.512(7)	O1-Eu1-O2	65.0(2)	La1-O1	2.335(6)	O1-La1-O2	125.3(2)
Eu1–O2	2.376(7)	O1-Eu1-O3	123.9(2)	La1–O2	2.485(6)	O1-La1-O3	115.0(2)
Eu1–O3	2.383(6)	O1-Eu1-O4	148.0(3)	La1–O3	2.457(6)	O1-La1-O4	72.6(2)
Eu1–O4	2.513(8)	O1-Eu1-O7	77.2(3)	La1–O4	2.449(6)	O1-La1-O5	63.9(2)
Eu1–O7	2.496(8)	O1-Eu1-O8	76.7(3)	La1–O5	2.339(6)	O1-La1-O6	64.96(19)
Eu1–O8	2.490(9)	O1-Eu1-O10	66.6(3)	La1–O6	2.500(6)	O1-La1-O8	120.5(3)
Eu1–O10	2.616(9)	O1-Eu1-O11	114.5(3)	La1–O8	2.491(9)	O1-La1–O9	168.3(3)
Eu1–O11	2.502(9)	O1-Eu1-O13	77.9(4)	La1–O9	2.615(10)	O1-La1-O11	70.5(4)
Eu1–O13	2.490(9)	O1-Eu1–O14	127.1(4)	La1–O11	2.463(13)	O1-La1–O12	106.3(4)
Eu1–O14	2.529(13)	O2-Eu1–O3	62.9(2)	La1–O12	2.439(9)	O2-La1-O3	76.2(2)
Cu1–O2	1.944(7)	O2-Eu1–O4	126.0(2)	Cu1–O1	1.977(6)	O2-La1-O4	77.4(2)
Cu1–O3	1.956(6)	O2-Eu1–O7	76.6(2)	Cu1–O5	1.951(6)	O2-La1-O5	65.2(2)
Cu1–O5	2.333(10)	O2-Eu1–O8	120.3(2)	Cu1–O15	2.334(9)	O2-La1-O6	147.11(19)
Cu1-N1	1.991(9)	O2-Eu1-O10	125.2(3)	Cu1-N1	1.974(7)	O2-La1-O8	113.5(3)
Cu1-N2	1.972(9)	O2-Eu1-O11	149.5(3)	Cu1-N2	1.995(7)	O2-La1–O9	65.8(3)
		O2-Eu1–O13	76.4(3)			O2-La1-O11	128.7(3)
		O2-Eu1-O14	88.3(3)			O2-La1–O12	78.3(4)
		O3-Eu1–O4	64.3(2)			O3-La1-O4	51.8(2)
		O3-Eu1–O7	72.0(2)			O3-La1-O5	120.6(2)
		O3-Eu1–O8	113.5(2)			O3-La1-O6	71.8(2)
		O3-Eu1–O10	169.1(3)			O3-La1-O8	85.3(3)
		O3-Eu1–O11	120.8(2)			O3-La1–O9	69.3(3)
		O3-Eu1–O13	108.1(3)			O3-La1-O11	147.7(4)
		O3-Eu1-O14	70.5(3)			O3-La1–O12	138.6(4)
		O4-Eu1-O7	77.2(3)			O4-La1-O5	76.2(2)
		O4-Eu1–O8	72.3(3)			O4-La1-O6	77.2(2)
		O4-Eu1–O10	108.7(3)			O4-La1-O8	133.1(2)
		O4-Eu1-O11	72.0(3)			O4-La1–O9	116.2(3)
		O4-Eu1-O13	131.9(3)			O4-La1-O11	142.8(4)
		O4-Eu1-O14	84.8(3)			O4-La1–O12	148.3(4)
		O7-Eu1–O8	50.5(3)			O5-La1-O6	127.2(2)
		O7-Eu1-O10	115.7(3)			O5-La1-O8	150.6(2)
		O7-Eu1-O11	133.8(3)			O5-La1–O9	124.4(3)
		O7-Eu1-O13	149.0(3)			O5-La1–O11	91.0(4)
		O7-Eu1–O14	142.4(4)			O5-La1–O12	75.3(4)
		O8-Eu1–O10	70.0(3)			O6-La1-O8	71.2(3)
		O8-Eu1–O11	87.2(3)			O6-La1–O9	108.2(3)
		O8-Eu1–O13	138.3(3)			O6-La1-O11	83.8(3)
		O8-Eu1-O14	150.3(4)			O6-La1-O12	132.1(4)
		O10-Eu1-O11	48.4(3)			O8-La1–O9	48.0(3)
		O10-Eu1-O13	69.7(4)			O8-La1-O11	66.6(4)
		O10-Eu1-O14	101.2(4)			O8-La1-O12	75.8(4)
		O11-Eu1-O13	74.0(4)			O9-La1-O11	100.0(4)
		O11-Eu1-O14	67.5(4)			O9-La1-O12	70.6(4)
		O13-Eu1-O14	50.8(4)			O11-La1-O12	51.2(5)
		O2-Cu1-N1	79.1(3)			O1-Cu1-N1	92.0(3)
		O2-Cu1-N2	91.6(3)			O1-Cu1-N2	167.9(3)
		O2-Cu1-O3	91.5(3)			O1-Cu1-O5	78.0(2)
		O2-Cu1-O5	168.2(3)			O1-Cu1-O15	94.2(3)
		O3-Cu1-O5	94.0(3)			O5-Cu1-O15	91.9(3)
		N1-Cu1-N2	168.2(3)			N1-Cu1-N2	96.8(3)
		O3-Cu1-N1	91.8(3)			O5-Cu1-N1	168.0(3)
		O3-Cu1-N2	93.3(4)			O5-Cu1-N2	92.3(3)
		O5-Cu1-N1	96.6(4)			O15-Cu1-N1	95.3(4)
		O5-Cu1-N2	96.6(4)			O15-Cu1-N2	93.2(3)
		Eu1-O2-Cu1	109.3(3)			La1–O1-Cu1	108.7(2)
		Eu1-O3-Cu1	108.6(3)			La1–O5-Cu1	109.4(3)

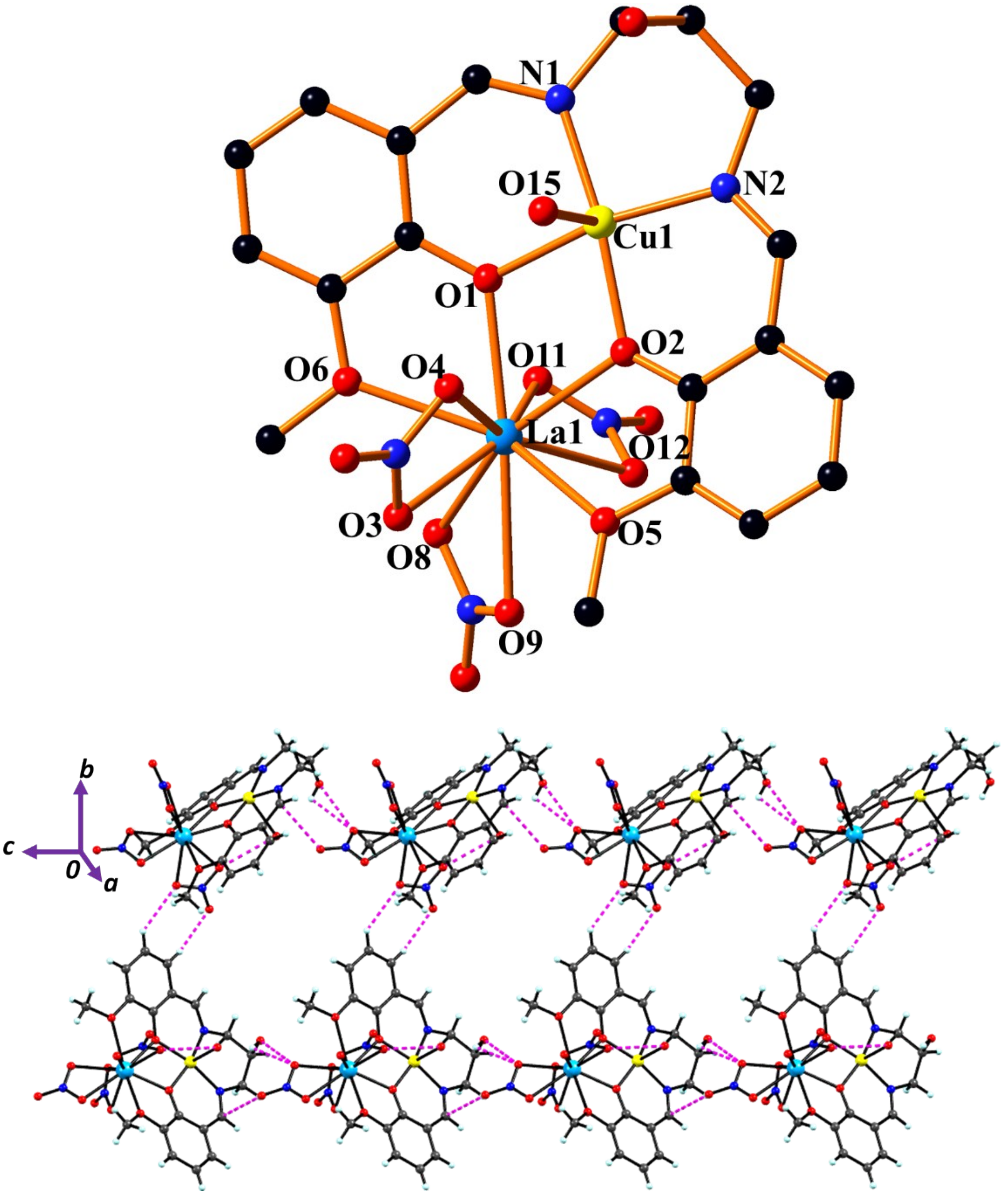

Figure S1 The molecular view of complex **2**; the supramolecular H-bonded 2D network (below) along crystallographic *bc* plane in complex **2**.

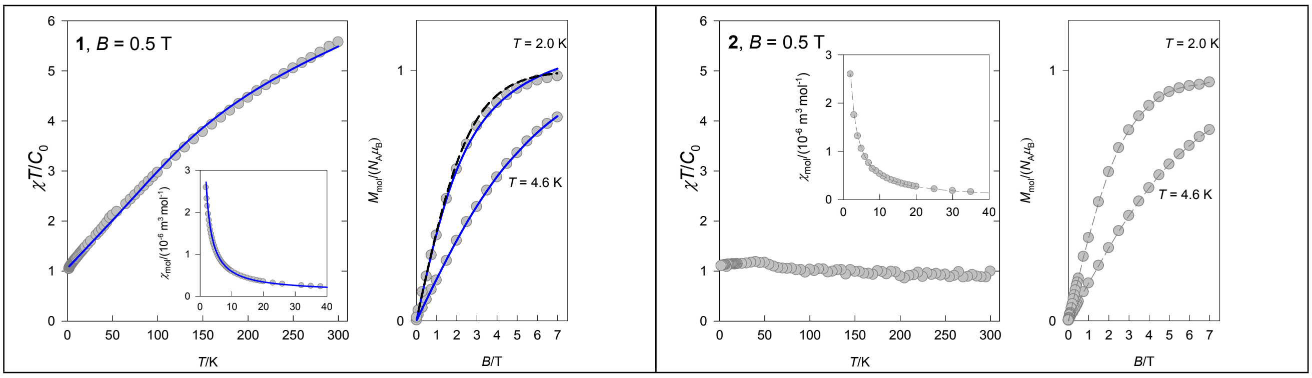

Figure S2 DC magnetic data.

Notes: $C_0 = N_A \mu_0 \mu_B^2 / k_B$, $C_0 = 4.71 \times 10^{-6}$ m^3 mol^{-1} (SI units) = 0.375 cm^3 mol^{-1} (cgs&emu units). $\chi T / C_0 = 1.0$ for the net $s = 1/2$ spin system obeying the Curie law.

AC susceptibility data

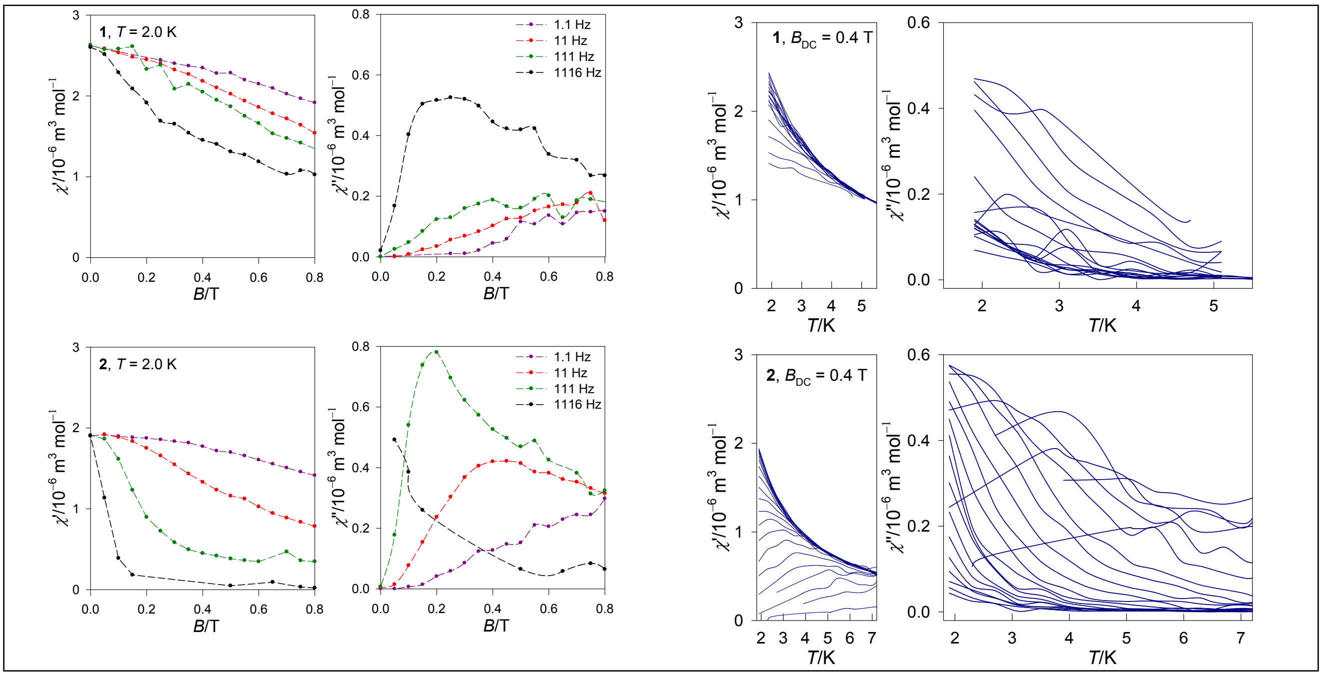

Figure S3 Comparison of the AC susceptibility components for **1** and **2**. Left – field dependence; right – temperature dependence.

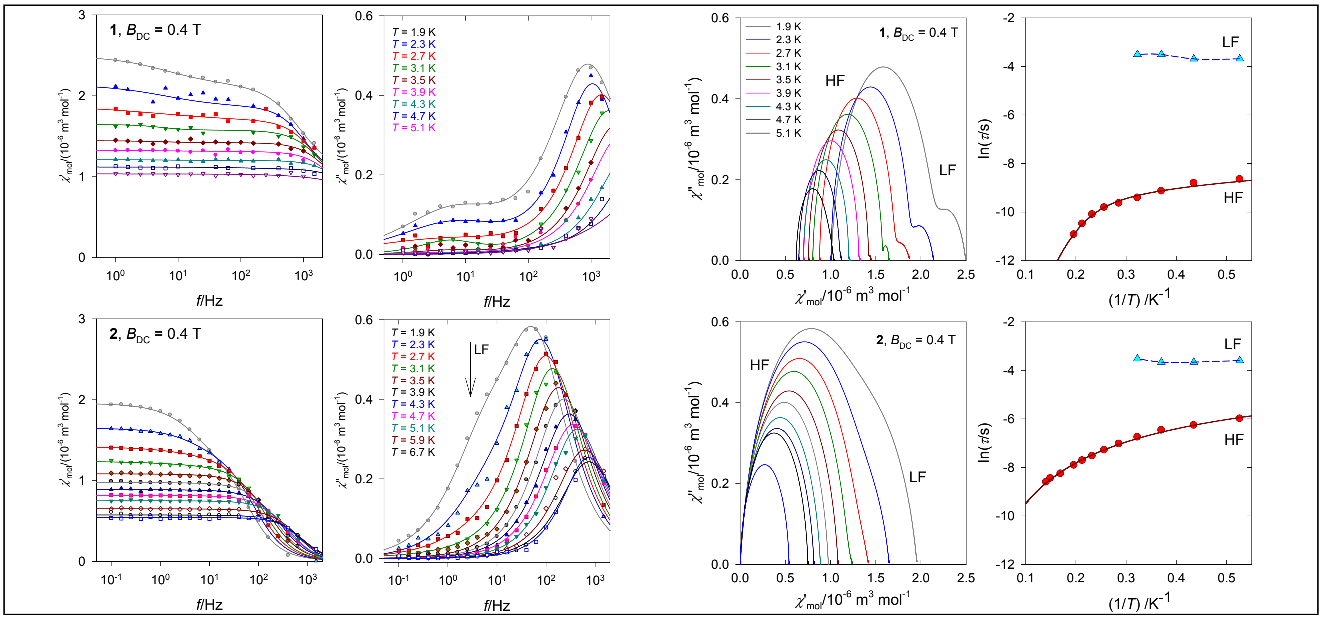

Figure S4. Collection of AC susceptibility data for **1** and **2** at B_{DC} = 0.4 T. Left – frequency dependence (lines – fitted with the two-set Debye model); right – Argand and Arrhenius-like plots.

Technical note: Some AC susceptibility data are uncommonly scattered owing to a weak signal arising from an $S = 1/2$ spin system and small amplitude of the AC field B_{AC} = 0.38 mT. Also fluctuations of the DC magnetic field raise the possible scattering. Each experimental point is an average of ten scans (each averaging four blocks) with omission of data outside 0.7σ interval. Time to average is as long as 79 s for f = 0.1 s.

Fitting of the AC susceptibility data is based upon 44 data points (22 in-phase and 22 out-of-phase) using the formula for the **two-set Debye model**

$$\chi(\omega) = \chi_S + \frac{\chi_{T1} - \chi_S}{1 + (\mathrm{i}\omega\tau_1)^{1-\alpha_1}} + \frac{\chi_{T2} - \chi_{T1}}{1 + (\mathrm{i}\omega\tau_2)^{1-\alpha_2}} \quad \text{or}$$

$$\chi(\omega) = \chi_S + (\chi_T - \chi_S)\left[\frac{x_1}{1 + (\mathrm{i}\omega\tau_1)^{1-\alpha_1}} + \frac{1 - x_1}{1 + (\mathrm{i}\omega\tau_2)^{1-\alpha_2}}\right]$$

where x_1 is the weight of the first, low-frequency relaxation set (channel, branch). This equation decomposes into two explicit formulae for
a) the in-phase component

$$\chi'(\omega) = \chi_S + (\chi_{T1} - \chi_S)\frac{1 + (\omega\tau_1)^{1-\alpha_1}\sin(\pi\alpha_1/2)}{1 + 2(\omega\tau_1)^{1-\alpha_1}\sin(\pi\alpha_1/2) + (\omega\tau_1)^{2-2\alpha_1}} + (\chi_{T2} - \chi_{T1})\frac{1 + (\omega\tau_2)^{1-\alpha_2}\sin(\pi\alpha_2/2)}{1 + 2(\omega\tau_2)^{1-\alpha_2}\sin(\pi\alpha_2/2) + (\omega\tau_2)^{2-2\alpha_2}}$$

b) the out-of-phase component

$$\chi''(\omega) = (\chi_{T1} - \chi_S)\frac{(\omega\tau_1)^{1-\alpha_1}\cos(\pi\alpha_1/2)}{1 + 2(\omega\tau_1)^{1-\alpha_1}\sin(\pi\alpha_1/2) + (\omega\tau_1)^{2-2\alpha_1}} + (\chi_{T2} - \chi_{T1})\frac{(\omega\tau_2)^{1-\alpha_2}\cos(\pi\alpha_2/2)}{1 + 2(\omega\tau_2)^{1-\alpha_2}\sin(\pi\alpha_2/2) + (\omega\tau_2)^{2-2\alpha_2}} \ \text{w}$$

ith the constraint for the isothermal susceptibilities $\chi_{T1} < \chi_{T2}$ in order to get positive contributions from each primitive component. Then $x_1 = (\chi_{T1} - \chi_S)/(\chi_{T2} - \chi_S) = (\chi_S - \chi_{T1})/(\chi_S - \chi_{T2})$.

Seven free parameters (χ_S, χ_{T1}, χ_{T2}, α_1, α_2, τ_1, and τ_2) can be fitted reliably by using 44 experimental data points. The functional to be minimized accounts to the relative errors of both susceptibility components

- $F = w \cdot E(\chi') + (1 - w) \cdot E(\chi'')$ with the typical weight $w = 0.07$, or
- $F = E(\chi') \cdot E(\chi'')$ with $E(\chi) = (1/N)\left[\sum_i^N \left|(\chi_i^{\mathrm{e}} - \chi_i^{\mathrm{c}})/\chi_i^{\mathrm{e}}\right|\right]$

Table S5 Fitted parameters of the Debye model for **1** and **2**.

a) **1** at $B_{\mathrm{DC}} = 0.4$ T

T/K	$R(\chi')$ /%	$R(\chi'')$ /%	χ_S	χ_{LF}	α_{LF}	τ_{LF} /10^{-3} s	χ_{HF}	α_{HF}	τ_{HF} /10^{-6} s
1.9	0.74	3.9	1.00(5)	1.37(9)	0.31(9)	25(4)	2.49(3)	0.12(3)	175(9)
2.3	3.0	4.0	1.00	1.29	0.34	25	2.14	0.01	150
2.7	2.8	6.5	0.88	1.06	0.50	30	1.87	0.01	108
3.1	1.3	5.3	0.80	0.87	0	30	1.64	0.04	82
3.5	1.2	15	0.76				1.32	0.00	63
3.9	1.4	15	0.70				1.33	0.02	55
4.3	1.0	17	0.70				1.21	0.00	41
4.7	1.1	18	0.65				1.11	0.00	28
5.1	1.4	41	0.62				1.03	0.00	18

b) **2** at $B_{\mathrm{DC}} = 0.4$ T

T/K	$R(\chi')$ /%	$R(\chi'')$ /%	χ_S	χ_{LF}	α_{LF}	τ_{LF} /10^{-3} s	χ_{HF}	α_{HF}	τ_{HF} /10^{-3} s
1.9	1.1	3.6	0	0.75(22)	0.25(5)	27(9)	1.96(1)	0.15(5)	2.5(3)
2.3	0.95	5.8	0	0.37	0.26	26	1.65	0.14	1.9
2.7	1.1	3.6	0	0.19	0.41	26	1.42	0.15	1.5
3.1	1.2	4.2	0	0.08	0.52	29	1.24	0.13	1.2
3.5	0.96	4.8	0				1.08	0.15	0.89
3.9	1.5	3.6	0				0.98	0.13	0.69
4.3	0.93	4.2					0.89	0.13	0.54
4.7	2.0	2.7					0.82	0.12	0.45
5.1	1.7	6.1					0.75	0.09	0.37
5.9	1.5	9.6					0.65	0.11	0.26
6.7	1.8	8.7					0.57	0.11	0.21
7.1	1.7	8.7					0.54	0.06	0.18

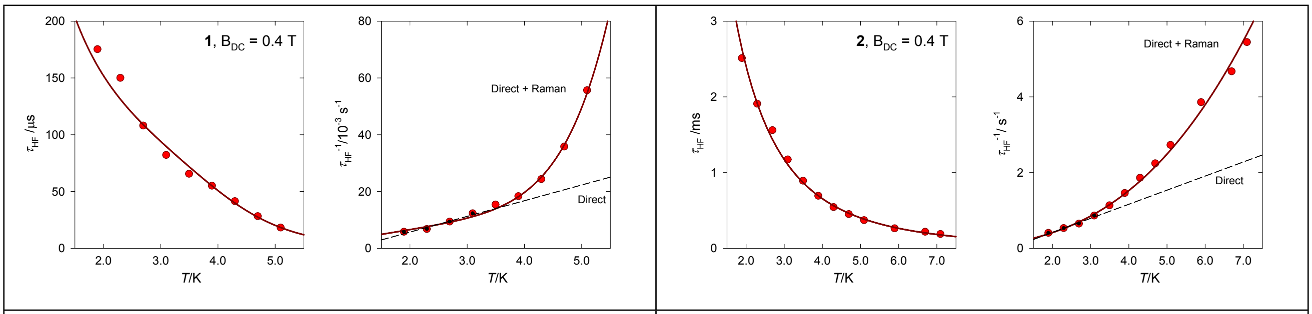

fitted with $A = 1.27(9) \times 10^{5}$ T^{-4} K^{-1} s^{-1},
$C = 0.29(27)$ K^{-n} s^{-1} and $n = 7.2$

fitted with $A = 5.1(31) \times 10^{3}$ T^{-4} K^{-1} s^{-1},
$C = 23(20)$ K^{-n} s^{-1} and $n = 2.7$

Figure S5 Plot of the HF relaxation rates for **1** and **2**; solid lines – fitted by $\tau^{-1} = AB^{4}T + CT^{n}$ referring to the direct and Raman relaxation processes.

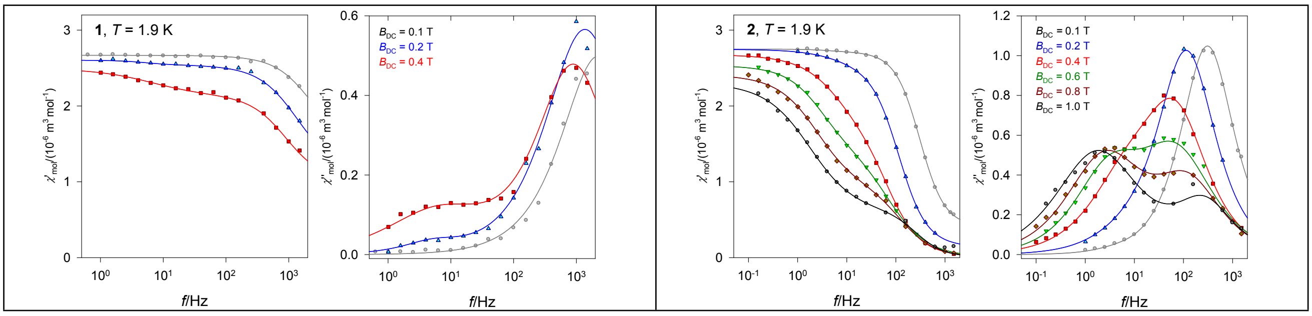

Figure S6 Field dependence of the AC susceptibility components at $T = 1.9$ K.

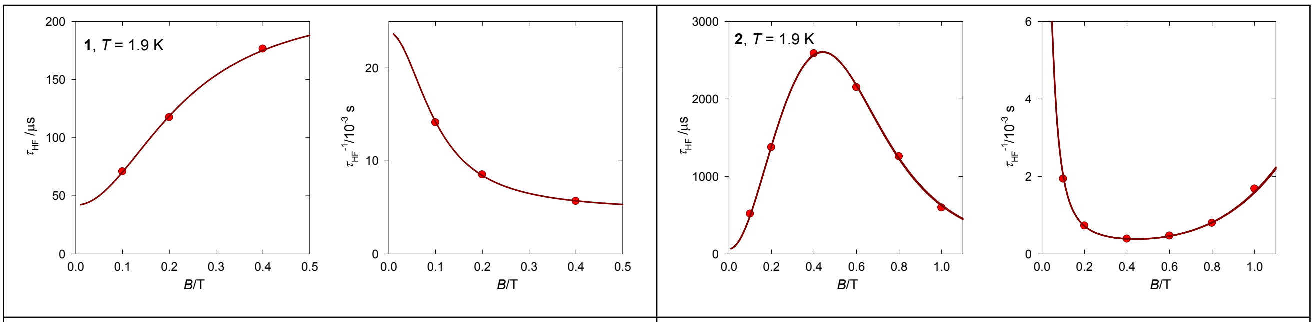

$$\tau^{-1} = D_1/(1 + D_2B^2) + D_3 :$$
$D_1 = 1.9 \times 10^{4}$ s^{-1}, $D_2 = 1.0 \times 10^{2}$ T^{-2},
$D_3 = 4.6 \times 10^{3}$ s^{-1}

$$\tau^{-1} = D_1/(1 + D_2B^2) + D_3 + A_TB^4 :$$
$D_1 = 1.6 \times 10^{4}$ s^{-1}, $D_2 = 7.8 \times 10^{2}$ T^{-2},
$D_3 = 2.3 \times 10^{2}$ s^{-1}, $A_T = 1.4 \times 10^{3}$ T^{-4} s^{-1}

Figure S7 Field dependence of the HF relaxation time at $T = 1.9$ K.

References:

1 M. Dolai, T. Mistri, A.Panja and M. Ali, *Inorg. Chim. Acta*, 2013, **399**, 95.
2 (a) SMART (V 5.628), SAINT (V 6.45a), XPREP, SHELXTL, Bruker AXS Inc., Madison, WI, 2004; (b) G. M. Sheldrick, SADABS (Version 2.03), University of Gottingen, Germany,2002.
3 (a) G. M. Sheldrick, SHELXS-97, Acta.Crystallogr., 2008, **A64**, 112; (b) A. L. Spek, Acta.Crystallogr., 2009, **D65**, 148.